

# INTERNATIONAL SCIENTIFIC CONFERENCE 20-22 November 2025, GABROVO



# BEND RADIUS (R/T) EFFECTS ON STRESS IN S355 SHEET BENDING: ELASTIC VS. ELASTOPLASTIC FINITE ELEMENT ANALYSIS

## Gürkan İRSEL

<sup>1</sup>Trakya University, Mechanical Engineering Department, Edirne, Turkey \*Corresponding author: gurkanirsel@trakya.edu.tr

#### **Abstract**

In this study, the effects of bend radius on stress concentration and permanent deformation in sheet metal geometries were numerically investigated using both elastic and elastic–plastic material models. Static analyses were conducted in ANSYS for ST52 (S355) steel plates with a constant thickness of 4 mm and various inner bend radii (R = 2, 4, 6, 8 mm). The material behavior was defined by a Multilinear Isotropic Hardening (MISO) model calibrated from tensile test data. Results showed that as the bend radius increased, the maximum equivalent stress decreased almost linearly. The mean stress was 390 MPa, with a standard deviation of 6.98 MPa and a strong negative correlation between R and stress (r = -0.994). The regression equation  $\sigma = -2.73R + 403.3$  (MPa) indicates a stress drop of approximately 2–3 MPa per mm radius increase. Elastic models produced unrealistic stresses exceeding the material's ultimate strength ( $\approx 670$  MPa), while the MISO-based elastic–plastic model realistically captured post-yield strain hardening and stiffness reduction. The activation of Large Deflection significantly improved deformation prediction under geometric nonlinearity, and Force Convergence evaluation confirmed stable and accurate nonlinear solutions. These results demonstrate that reliable FE analysis of sheet bending requires both plasticity modeling and geometric nonlinearity for physically meaningful stress prediction.

**Keywords:** Sheet Metal Bending, Bend Radius Effect, Elastic-Plastic Analysis, Plasticity, Finite Element Analysis (FEA).

#### INTRODUCTION

Bending of thin steel sheets is one of the most fundamental manufacturing operations in structural engineering and metal forming, extensively applied to produce load-bearing components in construction, automotive, and thin-walled structural assemblies where dimensional precision and residual strength are critical [1]. The mechanics of sheet bending are governed by the interplay between geometry (sheet thickness t, inner bend radius R, and R/t ratio), material constitutive behavior, and process boundary conditions. Small bend radii induce steep strain gradients through the thickness, localizing plastic flow near the outer fibers and generating high stress concentrations at the punch—die interface. Accurate prediction of these effects is therefore essential for ensuring manufacturability, springback control, and service reliability[2].

Finite element analysis (FEA) has become the principal tool for quantifying stress distribution, plastic strain localization, and residual curvature after unloading [3]. However, the fidelity of these predictions depends strongly on three interrelated modeling aspects:(1) constitutive representation of the material (isotropic vs. kinematic, bilinear vs. multilinear), (2) inclusion of geometric nonlinearity (small vs. large deflection), and (3) [4] refinement and element type (shell vs. solid, through-thickness resolution) [5].



Several studies have shown that purely elastic analyses yield unrealistic von Mises stress magnitudes, sometimes exceeding the ultimate tensile strength, because yielding and strain hardening are not captured. Conversely, experimentally calibrated Multilinear Isotropic Hardening (MISO) models accurately replicate post-yield behavior, ensuring physically meaningful stress—strain relationships and improved agreement with experimental data [6].

Material hardening representation is particularly critical. Isotropic hardening assumes uniform expansion of the yield surface with plastic strain and is simple to calibrate from uniaxial tensile tests, but it may underestimate unloading and reverse loading effects that influence springback. Combined isotropic-kinematic formulations, although more complex, provide superior predictions in cyclic bending-unloading scenarios. Recent works stress that calibration with true stress-true strain data—especially when represented with multilinear segments—substantially reduces discrepancies between FEA and experimental results, both in residual stress and permanent deformation predictions [7].

Geometric nonlinearity—commonly referred to as the Large Deflection effect plays a dominant role in accurately describing the deformation path of smallradius bends. When geometric nonlinearity neglected, load redistribution curvature evolution are misrepresented, leading to errors in both displacement and stress outcomes. Analytical and numerical studies, including those by and demonstrated that including geometric nonlinearity is indispensable for achieving realistic curvature evolution and ensuring solver stability via force convergence monitoring [3].

Mesh discretization is another decisive factor influencing accuracy. Shell elements are computationally efficient for global analyses but fail to capture throughthickness stress gradients, especially in fillet regions where strain localization dominates. High-order 3D solid elements (e.g., SOLID186) with fine local mesh refinement (0.25–0.5 mm) and controlled growth rates (≤1.15) deliver more accurate predictions for peak stress and plastic strain distribution. Mesh convergence studies have consistently shown that fine local refinement around bend radii and die–contact regions prevents artificial stress smoothing and ensures numerical stability[8][9].

Experimental investigations on S355 (ST52) structural steel indicate that the yield ( $\approx$ 355 MPa) and ultimate ( $\approx$ 670 MPa) along with moderate work strengths, hardening, produce significant residual stresses near sharp bend radii . These localized stresses can initiate fatigue cracking during cyclic service unless mitigated by proper forming parameters and residual stress management. This correlation between forming parameters, and fatigue behavior concentrations. underlines the need to integrate forming simulations with durability analyses[10].

Recent research efforts have also aimed to enhance numerical efficiency and model realism by incorporating hybrid modeling strategies. These include constitutive calibration using high-fidelity tensile data for MISO input, reduced-order modeling, and even machine learning surrogates trained on nonlinear **FEA** outputs. Nevertheless. despite computational advances, the reliability of such approaches fundamentally depends accurate plasticity representation and inclusion of geometric nonlinearity [8][11].

Despite the progress, two research gaps remain apparent. First, small-radius bending analyses of S355 steel using experimentally verified MISO curves and explicit force-convergence documentation are scarce in the literature. Second, many comparative studies neglect large-deflection effects or use inconsistent material parameters, hindering clear assessment of R/t influence and MISO calibration on stress evolution[6] [12].



Therefore, this study addresses these gaps through a comprehensive numerical investigation of the influence of bend radius (R = 2-8 mm) on the stress field of S355 structural steel (t = 4 mm). The material model employs a MISO curve calibrated from laboratory tensile tests, applied in both elastic and elastic–plastic static analyses under identical loading and boundary conditions. Geometric nonlinearity (Large Deflection) is activated, and convergence behavior is evaluated via Force Convergence criteria to ensure numerical stability.

Results are analyzed in terms of maximum equivalent (von Mises) stress, plastic strain distribution, and residual deformation, aiming to establish robust and reproducible modeling practices for sheet-bending simulations. The specific objectives and contributions of this study are summarized as follows:

- Quantitative determination of the peak equivalent stress-radius ( $\sigma_eq-R$ ) relationship for S355 sheets with t=4 mm and R=2, 4, 6, 8 mm.
- Demonstration of the necessity of MISO-based plasticity modeling for physically valid FEA predictions compared to elastic-only analyses[4].
- Evaluation of the Large Deflection effect on convergence behavior and geometric accuracy.
- Formulation of reproducible FEA modeling guidelines for thin-sheet bending, including local mesh sizing (0.25–0.5 mm), 10–12 inflation layers, and controlled growth rate (≤1.15)[5].

By systematically analyzing these aspects, the study contributes to both academic understanding and industrial application of reliable finite element modeling for small-radius sheet bending of structural steels.

# MATERIAL AND MODEL DEFINITION

The base material was selected as S355 (ST52) structural steel, whose mechanical properties were experimentally determined through tensile tests performed in accordance with ASTM E8 standards using a Zwick 600E (600 kN) universal testing machine (Fig. 1). The measured engineering stress–strain data were converted to true values and used to generate a Multilinear Isotropic Hardening (MISO) material model.

The MISO curve was defined by true stress—plastic strain data representing strain hardening behavior beyond the yield point. The experimentally determined parameters were:

- Yield strength = 355 MPa
- Ultimate tensile strength  $\approx 670 \text{ MPa}$
- Elastic modulus E = 210 GPa
- Poisson's ratio v = 0.3

This plasticity [4] model updates the stiffness matrix during each iteration, enabling the numerical analysis to accurately follow the deformation path observed experimentally (Table 1).



Fig. 1. Experimental tensile specimen used for calibration of the MISO model.



**Table 1.** True stress–plastic strain data defining the Multilinear Isotropic Hardening model.

Plastic Strain (mm/mm <sup>-1</sup> )	Stress (MPa)
0	355
0.0155	400
0.026	420
0.0296	440
0.0413	465
0.0574	489
0.08	528
0.113	572
0.143	593
0.164	607
0.188	624
0.206	634
0.226	638
0.241	641
0.3	642
1	645
2	660
10	670

#### **Geometric Modeling And Meshing**

The experimentally and numerically obtained tensile results showed strong agreement, particularly in the necking region, confirming the accuracy of the calibrated MISO model (Fig. 2).

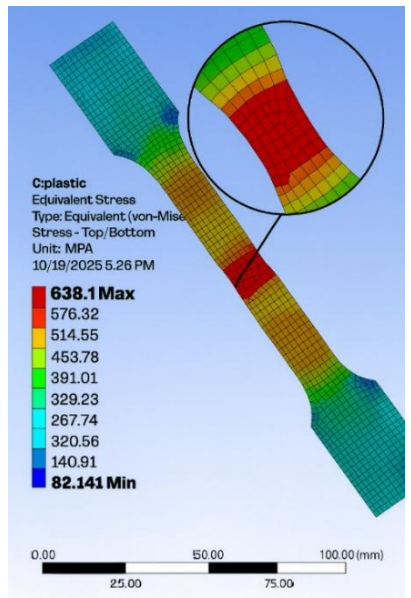


Fig. 2. Tensile test simulation verifying the MISO hardening model. The digital specimen reproduces necking behavior consistent with experiment.

All bending geometries were designed in CATIA Generative Sheet Metal Design using a constant sheet thickness of  $t=4\,\mathrm{mm}$  and inner radii  $R=2,\,4,\,6,\,\mathrm{and}\,8\,\mathrm{mm}$ . The modeled specimen dimensions were  $150\times59.3\,\mathrm{mm}$  (Fig. 3). One end was fully fixed, while a total load of 5 kN was applied at the opposite free edge. Although the geometry is thin-walled, 3D solid elements (SOLID186) were used instead of shell elements to capture through-thickness stress variations in the fillet regions.

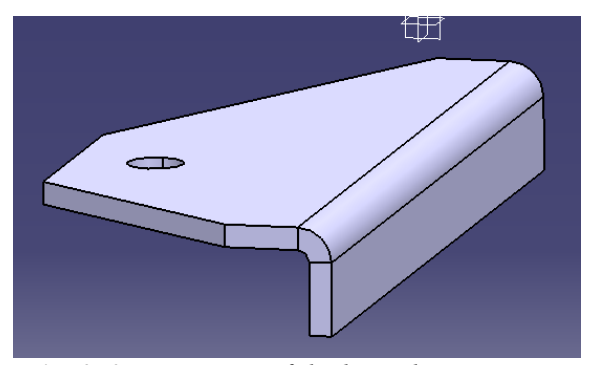


Fig. 3. 3D geometry of the bent sheet specimen created in CATIA Generative Sheet Metal Design, showing inner bend radius (R = 2-8 mm) and thickness (t = 4 mm).

A global element size of 2 mm was used, with local refinement applied in the radius zone down to approximately 0.25 mm to resolve high strain gradients. Inflation layers (10–12 layers, growth rate ≤ 1.15) were employed to improve accuracy through the sheet thickness. The generated mesh quality was verified, and the average skewness value remained below 0.36, ensuring accurate stress and strain representation throughout the model. showed that highorder 3D solid elements deliver more accurate stress distributions and springback estimates in small-radius V-bending than conventional shell meshes [5][13].

## **Nonlinear Solution Procedure**

In all analyses, Large Deflection was activated to include geometric nonlinearity. This option updates the stiffness matrix at each iteration, maintaining equilibrium





accuracy during large rotations. The Newton-Raphson iterative method was used for equilibrium at every load step (Fig. 4-7).

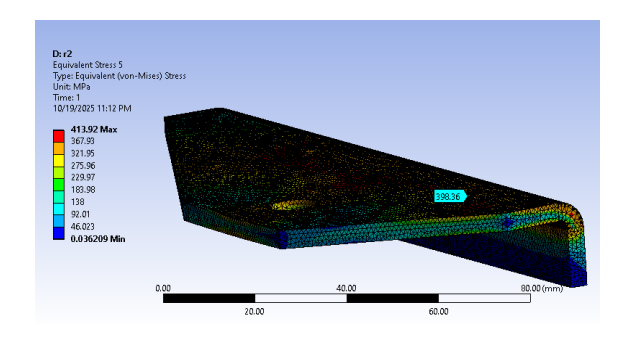


**Fig. 4** Equivalent von Mises stress distributions for bend radii (R = 2 mm).

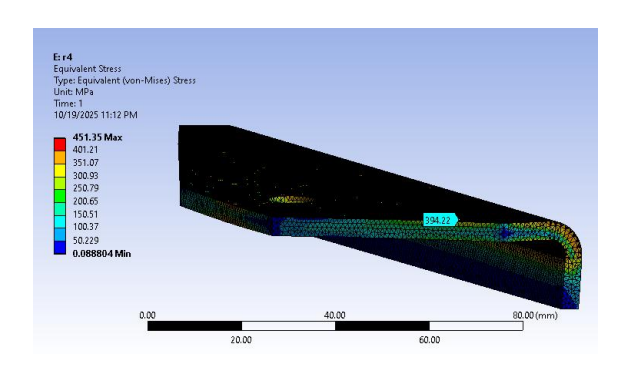


**Fig. 5** Equivalent von Mises stress distributions for bend radii (R = 4 mm).

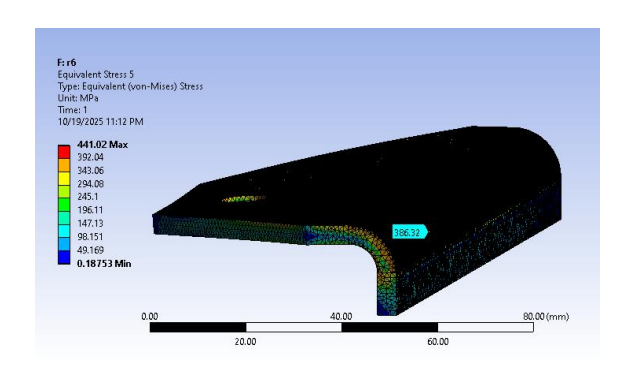


**Fig. 6** Equivalent von Mises stress distributions for bend radii (R = 6 mm).

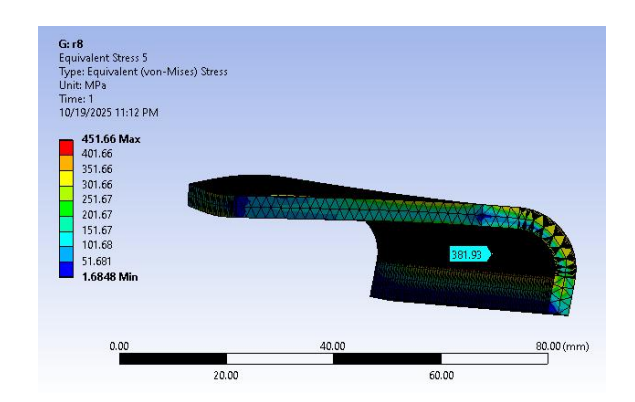


Fig. 7 Equivalent von Mises stress distributions for bend radii (R = 8 mm).

Whenever possible, three-dimensional (3D) models should be converted and analyzed in two-dimensional (2D) form, as this approach represents one of the most practical and effective methods for numerical verification and model validation.

In this context, the surface representation of the sheet model (R = 2 mm), originally analyzed in 3D, was generated, and a secondary analysis was conducted while maintaining the same MISO material definition, mesh density, and solution parameters (Fig. 8).

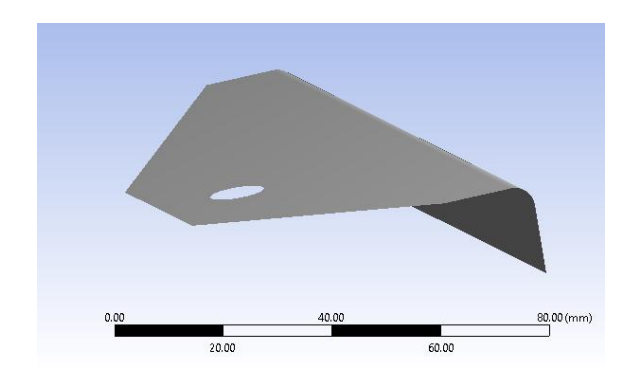


Fig. 8 2D geometry of the bent sheet specimen created in Space Claim

As a result of this comparative evaluation, the maximum equivalent stress obtained from the surface model was 399.62 MPa, demonstrating a high level of agreement with the 3D analysis results (Fig. 9).



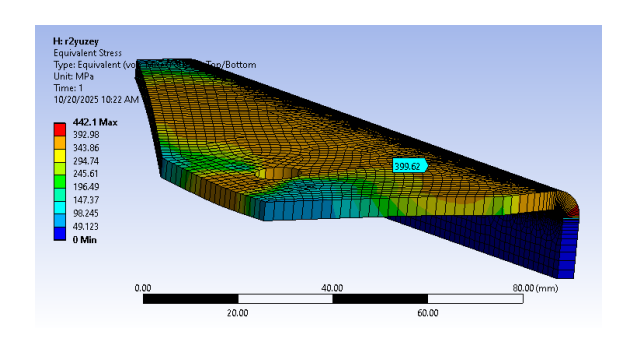


Fig. 9 Shell model stress analysis

When the same mesh and loading were analyzed without the MISO definition, the equivalent stress for R = 2 mm rose to 1185.9 MPa, far exceeding the ultimate strength of 670 MPa for S355 (Fig. 10).

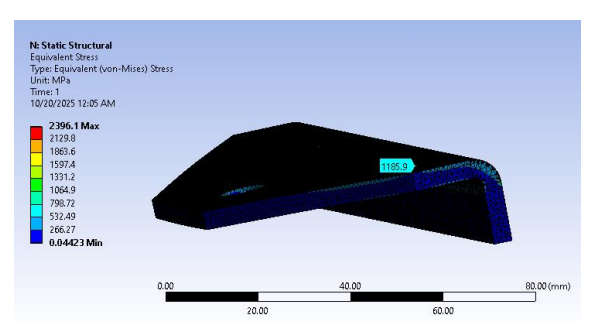
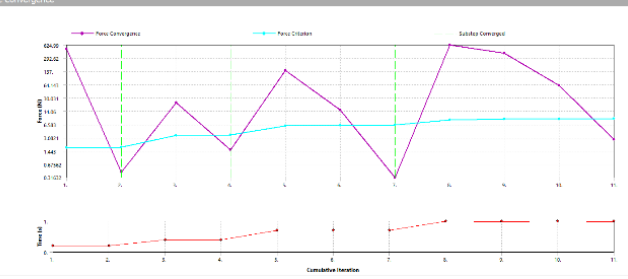


Fig. 10. Solution obtained with generic structural-steel definition (showing unrealistic 1185 MPa stress).

## Force-Convergence And Solver Behavior

All nonlinear runs converged within 11–13 iterations. Residual forces dropped from ~624 N to < 3 N per sub-step. Minor oscillations between iterations 3–5 corresponded to stiffness updates during plastic flow and curvature formation (Fig. 11).



**Fig. 11** Force convergence curve showing residual reduction and substep stability (11 iterations, 3 N threshold).

The ANSYS solution settings preferred and their effects are summarised in Table 2.

Table 2. Summary of solution-stability factors

Condition	Effect on Solution
Large Deflection = ON	Adds geometric nonlinearity; slight oscillations at curvature formation.
MISO Plasticity Active	Iterative stiffness updates; multiple equilibrium iterations.
Fine Mesh (0.5–1 mm)	Captures local gradients; improves stability at higher CPU time.

#### **RESULTS**

The finite element analysis performed using the MISO material definition for the tensile specimen demonstrated complete agreement with the experimental tensile test, both in terms of stress distribution and necking (plastic deformation) behavior (Fig. 12).

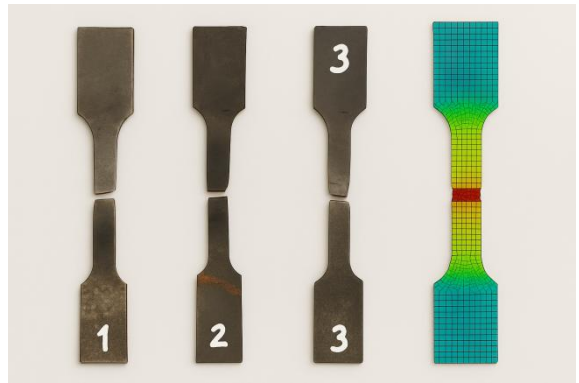


Fig. 12. Comparison of Experimental Tensile Specimens and Finite Element (FEM) Simulation Results under ASTM E8 Standard Validation

The 3D geometry of the bent sheet specimen was generated in CATIA Generative Sheet Metal Design, incorporating inner bend radii ranging from R = 2-8 mm and a constant thickness of t = 4 mm. Finite element analyses conducted on these models revealed that the maximum

"UNITECH – SELECTED PAPERS" vol. 2025 Published by Technical University of Gabrovo ISSN 2603-378X



equivalent (von Mises) stress decreases nearly linearly with increasing bend radius. For instance, at R=2 mm, the equivalent stress reached approximately 398 MPa, whereas at R=8 mm, it decreased to 382 MPa. The regression relationship between bend radius and maximum stress is presented in Table 3.

Table 3. Bend Radius-Stress Relation.

No	R (mm)	Max σ_eq (MPa)
1	2	398.36
2	4	394.22
3	6	386.32
4	8	381.93

The regression relation between bend radius and maximum stress was found as:

$$\sigma = -2.73R + 403.3$$

This indicates that an increase of 1 mm in radius results in a reduction of about 2.7 MPa in the peak stress.

The plastic strain contours indicated pronounced strain localization along the inner fillet for R=2-4 mm, while a nearly uniform strain distribution was observed for  $R\geq 6$  mm, consistent with increased triaxiality and local plastic flow at smaller radii . For the surface (2D) model analyzed under identical boundary and loading conditions, the equivalent von Mises stress at R=2 mm was obtained as 399.62 MPa. However, when the MISO plasticity definition was omitted, the corresponding stress value for the same radius increased unrealistically to 1185.9 MPa, exceeding the ultimate strength of S355 steel.

#### **DISCUSSION**

The comparative analyses clearly demonstrate that realistic finite-element (FE) predictions of sheet-bending behavior require both experimentally calibrated plasticity (MISO) and geometric nonlinearity (Large Deflection). When plasticity was neglected, the simulation produced a physically unrealistic peak stress

of 1185 MPa at R = 2 mm, exceeding the ultimate tensile strength of S355 (≈670 MPa). Conversely, the MISO-based model reproduced the true stress–strain response and necking behavior observed experimentally, validating its physical accuracy [14].

The force-convergence behavior across all nonlinear runs exhibited high stability. Residual forces dropped below 3 N within 11–13 iterations, indicating proper equilibrium and solver robustness. Likewise, monitoring Newton–Raphson convergence provides quantitative assurance of solver stability in nonlinear analyses [8].

Verification of mesh independence was achieved through a 2D–3D comparison: the 3D analysis produced a maximum stress of 398.36 MPa, while the 2D surface model yielded 399.62 MPa—a difference below 0.3%. This consistency confirms the adequacy of the selected mesh parameters (local size 0.25–0.5 mm, 10–12 inflation layers, growth  $\leq$ 1.15). The average mesh skewness of 0.36 remained within high-quality bounds for reliable stress-gradient capture.

The bend-radius parameter (R) exhibited only a limited mechanical influence on stress levels. The nearly linear stress decrease of  $\approx$ 2.7 MPa/mm resulted in a total variation of <5% between R = 2 mm and R = 8 mm. This minor effect indicates that manufacturing and tooling considerations should take precedence over theoretical stress minimization [1].

The activation of Large Deflection significantly improved geometric accuracy by accounting for curvature-induced nonlinearities. Without it, curvature evolution and stress redistribution become unrealistic even with accurate material laws. In the present study, the joint use of MISO and geometric nonlinearity produced stable convergence (<3 N residual) and physically consistent strain localization.

From a manufacturing standpoint, these results confirm that bend-radius selection



should primarily depend on tooling configuration, geometry, die and dimensional-accuracy requirements, since the minor stress differences among R values are mechanically negligible. The findings also validate that MISO-based plasticity, Large Deflection, and high-quality meshing collectively establish a numerically robust and experimentally consistent modeling framework for small-radius sheet bending of structural steels [2].

#### **CONCLUSIONS**

- Increasing bend radius lowers peak von Mises stress nearly linearly; for 4-mm S355,  $\sigma \approx -2.73R + 403.3$  MPa ( $\approx 2.7$  MPa drop per 1 mm, R=2-8 mm).
- Purely elastic analysis is non-physical: at R=2 mm, ≈1185.9 MPa exceeds ~670 MPa UTS; MISO elastoplasticity is required.
- Enable geometric nonlinearity (Large Deflection); combined with MISO it yields stable convergence and physically consistent deformation.
- Nonlinear runs are stable: residual forces ≤3 N per substep with convergence in 11–13 iterations.
- 2D vs. 3D models differ by <0.3% in peak stress (398.36 vs. 399.62 MPa), validating the faster 2D option.
- Mesh quality is critical: fillet refinement ~0.25–0.5 mm, 10–12 inflation layers, growth ≤1.15, average skewness <0.36.</li>
- The calibrated MISO curve (σy≈355 MPa, UTS≈670 MPa; E=210 GPa, v=0.3) reproduces tensile necking and post-yield hardening in bending.
- Bend radius affects stress modestly (<5%); prioritize die geometry, precision, and tolerances. MISO + Large Deflection + quality meshing provides a repeatable, industry-ready FEA workflow.

#### **ACKNOWLEDGMENT**

This study was supported by Matil Materials Testing and Innovation Laboratories Inc.and Becan Machinery Inc., who provided experimental facilities and prototype validation support.

#### REFERENCES

- [1] C. Zhang and Y. Lou, "Influences of the evolving plastic behavior of sheet metal on V-bending and springback analysis considering different stress states," Int. J. Plast., vol. 173, no. December 2023, p. 103889, 2024, doi: 10.1016/j.ijplas.2024.103889.
- [2] B. S. Levy and C. J. Van Tyne, "Predicting breakage on a die radius with a straight bend axis during sheet forming," J. Mater. Process. Technol., vol. 209, no. 4, pp. 2038–2046, 2009, doi: 10.1016/j.jmatprotec.2008.04.053.
- [3] M. Knezevic, "Crystal plasticity-based finite element simulations of load reversals and hat-shaped draw-bending for predicting the springback behavior of dual-phase steel sheets," Int. J. Solids Struct., vol. 300, no. July 2023, p. 112924, 2024, doi: 10.1016/j.ijsolstr.2024.112924.
- [4] D. C. Feng, G. Wu, Z. Y. Sun, and J. G. Xu, "A flexure-shear Timoshenko fiber beam element based on softened damage-plasticity model," Eng. Struct., vol. 140, pp. 483–497, 2017, doi: 10.1016/j.engstruct.2017.02.066.
- [5] P. Solfronk, J. Sobotka, and D. Koreček, "Effect of the Computational Model and Mesh Strategy on the Springback Prediction of the Sandwich Material," Machines, vol. 10, no. 2, 2022, doi: 10.3390/machines10020114.
- [6] B. N. Fetene, R. Shufen, and U. S. Dixit, "FEM-based neural network modeling of laser-assisted bending," Neural Comput. Appl., vol. 29, no. 6, pp. 69–82, 2018, doi: 10.1007/s00521-016-2544-9.
- [7] A. P. Agrawal, S. Ali, and S. Rathore, "Finite element stress analysis for shape optimization of spur gear using ANSYS," Mater. Today Proc., vol. 64, pp. 1147–1152, 2022, doi: 10.1016/j.matpr.2022.03.404.



- [8] M. T. Ozkan and F. Erdemir, "Determination of theoretical stress concentration factor for circular/elliptical holes with reinforcement using analytical, finite element method and artificial neural network techniques," Neural Comput. Appl., vol. 33, no. 19, pp. 12641–12659, 2021, doi: 10.1007/s00521-021-05914-x.
- [9] L. Zhang et al., "Active shovel spinning process: Plastic deformation behavior, microstructure, and properties," Thin-Walled Struct., vol. 206, no. PC, p. 112714, 2025, doi: 10.1016/j.tws.2024.112714.
- [10] Y. M. Huang, "Finite element analysis on the V-die coining bend process of steel metal," Int. J. Adv. Manuf. Technol., vol. 34, no. 3–4, pp. 287–294, 2007, doi: 10.1007/s00170-007-1054-4.
- [11] S. Ibáñez and M. Kraus, "Numerical method for the primary torsional capacity of arbitrary steel cross sections considering nonlinear plastic behaviour," Results Eng.,

- vol. 22, no. February, 2024, doi: 10.1016/j.rineng.2024.102172.
- [12] D. Xu, J. Chen, Y. Tang, and J. Cao, "Topology optimization of die weight reduction for high-strength sheet metal stamping," Int. J. Mech. Sci., vol. 59, no. 1, pp. 73–82, 2012, doi: 10.1016/j.ijmecsci.2012.03.006.
- [13] M. Vivet, D. Mundo, T. Tamarozzi, and W. Desmet, "An analytical model for accurate and numerically efficient tooth contact analysis under load, applied to face-milled spiral bevel gears," Mech. Mach. Theory, vol. 130, pp. 137–156, 2018, doi: 10.1016/j.mechmachtheory.2018.08.016.
- [14] S. Bayramoglu, S. Akpinar, and A. Çalık, "Numerical analysis of elasto-plastic adhesively single step lap joints with cohesive zone models and its experimental verification," J. Mech. Sci. Technol., vol. 35, no. 2, pp. 641–649, 2021, doi: 10.1007/s12206-021-0124-0.